Available online at www.sciencedirect.com
SCIENCE DIRECT®
International Journal of Multiphase Flow 31 (2005) 1036–1048
International Journal of Multiphase Flow
www.elsevier.com/locate/ijmulflow

Comparison of results from DNS of bubbly flows with a two-fluid model for two-dimensional laminar flows

Souvik Biswas, Asghar Esmaeeli, Gretar Tryggvason *

Mechanical Engineering Department, Worcester Polytechnic Institute, 100 Institute Road, Worcester, MA 01609-2280, United States

Received 10 February 2005; received in revised form 17 April 2005

Abstract

Results from direct numerical simulations of laminar bubbly flow in a vertical channel are compared with predictions of a two-fluid model for steady-state flow. The simulations are done assuming a two-dimensional system and the model coefficients are adjusted slightly to match the data for upflow. The model is then tested by comparisons with different values of flow rate and gravity, as well as downflow. In all cases the results agree reasonably well, even though the simulated void fraction is considerably higher than what is assumed in the derivation of the model. The results do, however, suggest a need to understand the lift and the wall repulsion force on bubbles better, particularly in dense flows.

Keywords: Bubbly flow; Direct numerical simulations; Two-fluid model

1. Introduction

The goal of direct numerical simulations (DNS) of disperse bubbly multiphase flows, where every continuum length and time scale is fully resolved, is twofold: Such simulations should generate insight and understanding of the basic behavior of the flow, including the forces on

* Corresponding author. Tel.: +1 508 831 5759; fax: +1 508 831 5680.
E-mail address: gretar@wpi.edu (G. Tryggvason).

0301-9322/$ - see front matter © 2005 Elsevier Ltd. All rights reserved.
doi:10.1016/j.ijmultiphaseflow.2005.06.002

the bubbles, how the bubbles affect the flow, and how many bubbles interact in dense disperse flows. Secondly, the vast data generated by direct numerical simulations should help in the construction of closure models for engineering simulations of the averaged flow field. As in turbulent flow of a single-phase fluid, multiphase flows generally possess a large range of scales, ranging from the sub-millimeter size of a small bubble or an eddy to the size of the system under investigation. For an industrial bubble column or the flow around a ship, the ratio of the smallest to the largest scale is easily tens or hundreds of thousands. Assume, somewhat arbitrarily, that we need of the order of 10 grid points per smallest scale, that the smallest bubble or eddy is about a millimeter, and that we need to simulate a system whose dimensions are measured in meters. For this relatively modest system we would need over 10^{12} grid points. While simulating such systems is likely to be possible within 10–20 years, particularly if adaptive gridding can be used to reduce the actual number of grid points used, it is unlikely that it will be practical to use such huge simulations for routine engineering predictions. For reference we note that a simulation of homogeneous turbulence using 4096^3 modes has recently been reported in Kaneda et al. (2003). Furthermore, it is likely that this will not be necessary, except in a few special cases. Multiphase flows, like single-phase turbulent flows, exhibit a great deal of universality at the smallest scales and it is almost certain that re-computing small-scale behavior that is already understood is not necessary. Thus, it is likely that models of multiphase flows, where the average motion is computed, but the influence of small, unresolved scales is accounted for by closure models, will be in use for the foreseeable future. Providing accurate closure models will therefore continue to be at the center of multiphase flow research.

Equations for the average behavior of multiphase systems can take several forms. The simplest assumption is that the multiphase flow is a mixture whose properties depend on the void fraction. In the mixture approximation there is a single average velocity, but in most cases the bubbles and the liquid move with different velocities and the behavior of the flow depends strongly on the slip velocity between the bubbles and the liquid. Today it is therefore most common to work with "two-fluid models" where separate mass and momentum (and energy where appropriate) equations are written for the different fluids. The liquid motion is almost always computed by continuum equations resembling the Navier–Stokes equations but containing additional terms accounting for the presence of the bubbly phase. The motion of the bubbles can be computed by a similar continuum equation (the "Euler–Euler" approach) or by representing the bubbles (or an assembly of bubbles) by marker points that move through the liquid (the "Euler–Lagrangian" approach). Both approaches are commonly used (Drew and Passman, 1999; Crowe et al., 1998). For very low void fraction and very small particles, it is sometimes possible to ignore the effect of the bubbles on the liquid (one-way coupling), but in most cases the effect of the bubbles on the liquid must be accounted for (two-way coupling). The equations for the averaged motion of the liquid contain two terms that represent the effect of the bubbles. One is the force that the bubbles exert on the liquid and the other is the velocity fluctuations generated by the motion of the bubbles. Nonuniform bubble distribution can also lead to buoyancy driven currents and in turbulent bubbly flow the bubbles can modify the turbulence and thus the evolution of the flow.

Here, we examine the applicability of a simple two-fluid model to a flow that can be examined by direct numerical simulations relatively easily. We consider a two-dimensional laminar flow in a vertical channel and compare the results with predictions obtained using a two-fluid model. The key questions are how well the model, derived using small bubbles and a dilute flow, performs

in situations that are easily simulated (large bubbles and dense flow), and how large a system needs to be and for how long the evolution must be simulated to reach an approximate steady state that can be compared with the two-fluid model?

2. Problem setup and numerical model

We examine the steady state flow of bubbles in a vertical channel, with gravity acting downward parallel to the walls, for both up and downflow. See Fig. 1, where we define the vertical coordinate as y and x as the cross-channel coordinate. The flow is driven by a pressure gradient in the y-direction, but on the average the flow is assumed to be homogeneous in that direction. Therefore $\partial/\partial y = 0$ (except that $\mathrm{d}p/\mathrm{d}y = \text{constant}$). The flow in the channel is characterized by the Reynolds number without bubbles. Here, we shall limit our considerations to systems with bubbles of only one size, so the bubble motion is determined by the Archimedes number, N, and the Eötvös number, Eo. In addition, we need to specify either the number of bubbles n_b or the void fraction, ε. The governing nondimensional numbers therefore are:

$$Re_\mathrm{ch} = \frac{\rho_\mathrm{L} H U}{\mu_\mathrm{L}}; \quad Eo = \frac{\rho_\mathrm{L} d_\mathrm{e}^2 g}{\sigma}; \quad N = \frac{\rho_\mathrm{L}^2 d_\mathrm{e}^3 g}{\mu_\mathrm{L}^2}; \quad \varepsilon = n_\mathrm{b} \pi \frac{d_\mathrm{e}^2}{4}$$

Here H is the width of the channel, U is the average velocity in the channel before the bubbles are added, ρ_L and μ_L, are the liquid density and viscosity, respectively, σ is the surface tension, g is the gravity acceleration, n_b is the number density of bubbles, and d_e is diameter of the (undeformed) bubbles.

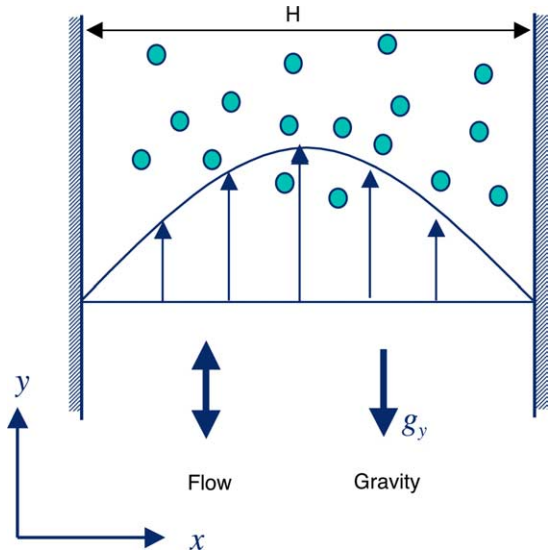

Fig. 1. The problem setup. The flow is fully developed and at steady-state. The width of the channel is H, the average velocity in the absence of bubbles is U, gravity acts in the negative y-direction and the pressure gradient is selected to generate either up or downflow.

The simulations, where the unsteady motion of the bubbles is computed by fully resolving all flow scales, were carried out by a finite-volume/front tracking technique where one set of equations is used for the whole domain, including both the bubbles and the carrying liquid. The bubble surface is explicitly marked by connected marker points that move with the flow and are used to update the density and viscosity at each grid point and to find the surface tension. The method is described in detail in Tryggvason et al. (2001).

3. The two-fluid model

The two-fluid model that we examine here is based on writing separate conservation equations for each phase. By assuming a fully developed, steady-state flow, and that the density of the bubble phase can be neglected, Antal et al. (1991) derived a model for laminar bubbly flow in a circular pipe. For the two-dimensional flow in Fig. 1, the corresponding equations are

$$\varepsilon\frac{\mathrm{d}p_\mathrm{G}}{\mathrm{d}y}+\varepsilon\rho_\mathrm{G}g_y=-\frac{3}{8}\frac{\varepsilon}{R_\mathrm{b}}C_\mathrm{D}\rho_\mathrm{L}U_\mathrm{r}|U_\mathrm{r}| \tag{1}$$

$$(1-\varepsilon)\frac{\mathrm{d}p_\mathrm{L}}{\mathrm{d}y}+(1-\varepsilon)\rho_\mathrm{L}g_y=(1-\varepsilon)\mu_\mathrm{L}\frac{\partial^2 u_\mathrm{L}}{\partial x^2}+\frac{3}{8}\frac{\varepsilon}{R_\mathrm{b}}C_\mathrm{D}\rho_\mathrm{L}U_\mathrm{r}|U_\mathrm{r}| \tag{2}$$

$$\varepsilon\frac{\partial\varepsilon}{\partial x}\frac{|U_\mathrm{r}|^2}{5}(1-\varepsilon)=-\varepsilon C_\mathrm{L}U_\mathrm{r}\frac{\partial u_\mathrm{L}}{\partial x}-\varepsilon\left(C_\mathrm{w1}+C_\mathrm{w2}\frac{R_\mathrm{b}}{s}\right)\frac{U_\mathrm{r}^2}{R_\mathrm{b}} \tag{3}$$

Here, $\varepsilon=\varepsilon_\mathrm{G}=1-\varepsilon_\mathrm{L}$ is the void fraction of the air, U_r is the relative velocity of the bubbles with respect to the liquid, and u_L is the liquid velocity in the vertical direction. The density and viscosity of the liquid are ρ_L and μ_L, respectively, and g_y is the gravity acceleration. The drag coefficient in (1) is given by

$$C_\mathrm{D}=\frac{24}{Re}(1+0.1Re^{0.75}) \tag{4}$$

where the Reynolds number and the effective viscosity are given by

$$Re=\frac{2R_\mathrm{b}\rho_\mathrm{L}|U_\mathrm{r}|}{\mu_\mathrm{m}},\quad \mu_\mathrm{m}=\frac{\mu_\mathrm{L}}{1-\varepsilon} \tag{5}$$

The pressure gradients in the gas and the liquid are taken to be equal and given and we use the average void fraction when computing the Reynolds number in Eq. (5). The first equation is the momentum conservation equation for the gas phase in the vertical direction (y), where the vertical pressure gradient and the weight of the liquid are balanced by the drag force due to the bubbles. The second equation is the vertical momentum equation for the liquid phase showing that the vertical pressure gradient and the weight of the liquid on the left hand side are balanced by the liquid shear and the drag force from the bubbles on the right hand side. The third equation is the gas momentum equation in the horizontal direction (x), where the bubble advection (left hand side) is balanced by the lift force (first term on the right) and the wall repulsion force. The wall repulsion (last term on the right) is given by the model of Antal et al. (1991). Here s is the distance to

the closest wall and the wall repulsion force, which is always away from the wall, is set to zero for s large enough to yield a force toward the wall. The coefficients used here are taken from Azpitarte and Buscaglia (2003) who used: $C_{w1} = -0.106$, $C_{w2} = 0.147$ and $C_L = 0.05$.

To solve these equations we discretize the domain using 501 grid points, which is more than enough to give fully converged results for the parameters examined here. Initially, we assume that the void fraction is a constant and the liquid velocity is zero. We start by solving Eq. (1) for U_r. Then Eq. (2) is solved implicitly using a tri-diagonal solver to find $u_L(x)$ and finally Eq. (3) gives $\varepsilon(x)$ by marching from one wall to the other. The new ε is then used to solve Eq. (2) again for the liquid velocity, Eq. (3) gives a new void fraction and so on, iteratively until the solution has converged. For the solution of Eq. (2) we use the boundary conditions $u_L(0) = u_L(H) = 0$. After the solution has converged, $\varepsilon(x)$ is corrected to conserve ε, i.e.

$$\varepsilon^{new}(x) = \varepsilon(x) + \varepsilon_0 - \frac{1}{H}\int_0^H \varepsilon(x)\,dx \tag{6}$$

where ε_0 is the specified average void fraction. This generally results in negative values for the void fraction near the walls and in the plots of $\varepsilon(x)$ we replace the negative values by zero.

4. Results

Fig. 2 shows the bubble distribution and the velocity field at a late time for two simulations of 72 bubbles. Here $Eo = 0.5$, $M = Eo^3/N^2 = 1.25 \times 10^{-5}$, and the diameter of the initially circular bubbles is $0.08 \times H$, resulting in $\varepsilon_0 = 0.1206$. The channel Reynolds number without bubbles is $Re = 823.51$. The length of the computational domain is three channel widths and we impose periodic boundary conditions in the streamwise direction. The domain is resolved by a 256×769 grid, except for the two cases with smaller bubbles (discussed later) where we used a 384×1152 grid. Grid refinement studies have shown that this resolution results in essentially fully converged solution. The simulation for the upflow case discussed below took slightly less than 5 days on one dedicated Intel(R) Xeon 2.40 GHz processor (35,381 time steps, up to nondimensional time 75.0). Other runs took comparable times. For computational convenience we take the bubble density and viscosity to be one twentieth of the liquid. As discussed by Esmaeeli and Tryggvason (1999), reducing the density and viscosity of the bubbles has essentially no impact on the results. In the frame on the left the pressure gradient is set to generate upflow and for the right frame the pressure gradient is reversed, resulting in downflow. The flow is initially started using the velocity profile predicted by the two-fluid model for these parameters, but the bubbles are uniformly distributed across the channel. Since gravity acceleration points downward, the bubbles rise upward, relative to the liquid, in both cases. For the upflow the liquid velocity increases the rise of the bubbles and for the downflow the liquid flow slows them down, relative to a stationary observer. The fluid shear near the walls has a different sign for the different flow directions. Since the bubbles remain essentially cylindrical, even in the high shear region near the walls, the lift of a bubble rising relative to the liquid is toward the slow moving fluid. Thus, the lift force will push a bubble toward the wall for upflow and toward the middle of the channel for downflow. In most of the channel, however, the void fraction and the velocity are relatively uniform and the effect of lift is therefore not as strong as one might initially suspect. Indeed, the distribution of the bubbles

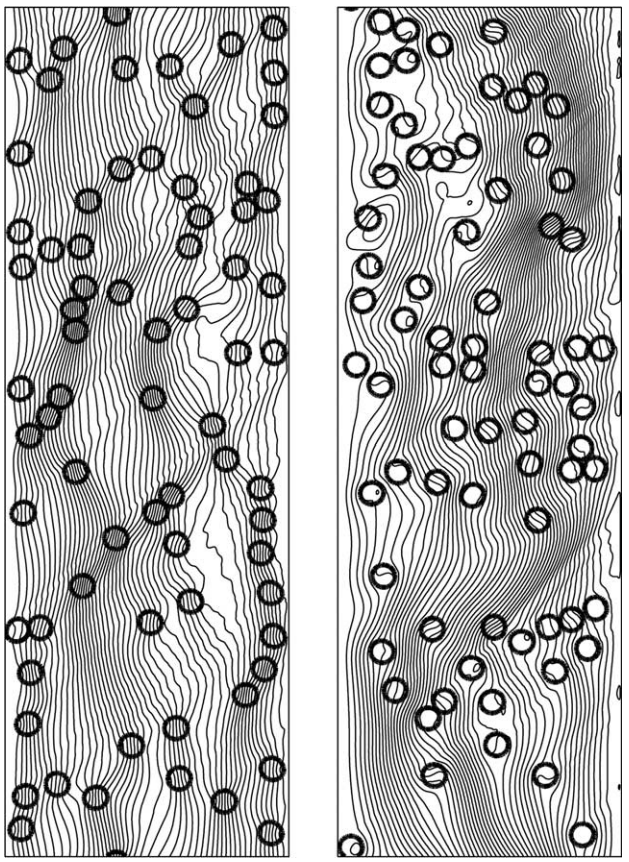

Fig. 2. Two simulations of the rise of bubbles in upflow in a vertical channel (left frame) and downflow (right frame). The bubbles and the streamlines in a stationary frame of reference are shown at a late time after the flow has reached a statistically steady-state.

in Fig. 2 do not look fundamentally different, although we will see below that there is, on the average, a larger number of bubbles near the walls for the upflow than for the downflow. For the downflow we do, in particular, not see bubbles hugging the walls for long periods of time as we see for the upflow.

To quantify the evolution of the flow, and to assess whether the flow is at steady-state, we plot in Fig. 3 the average rise Reynolds number of the bubbles versus time (a), the average through flow (b), and the average root mean squared (rms) distance of the bubbles from the centerline of the channel (c). In both cases the flow has reached a relatively well-defined steady-state, but the upflow case shows a significantly longer transient and may be undergoing small long-time oscillations. Since the number of bubbles is relatively small, the average bubble velocity shows higher frequency fluctuations than the through flow, which is found by integrating over the whole domain. The relatively uniform distribution of the bubbles is clear in the rms distance of bubbles from the centerline (c), where we see that although the bubbles in upflow are closer to the walls, the difference is relatively small.

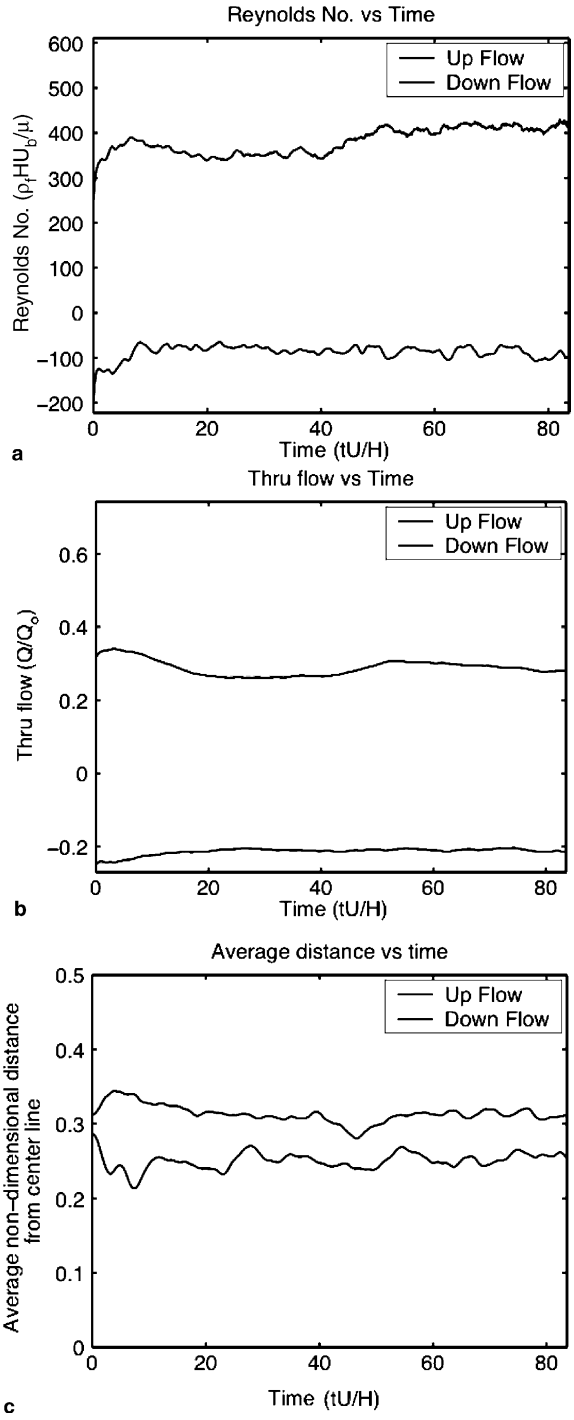

Fig. 3. The average bubble rise Reynolds number (a), the through flow normalized by the channel flow without bubbles (b) and the root-mean-squared distance of the bubbles from the centerline of the channel, normalized by half the channel width (c).

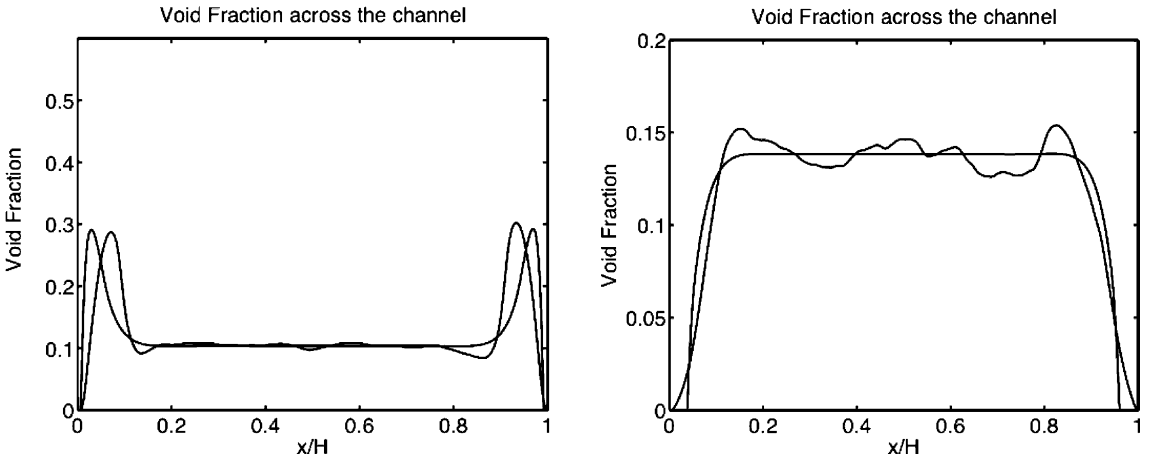

Fig. 4. The averaged void fraction profile from the simulations and as predicted by the two-fluid model, using the original values for the model coefficients. Results for upflow are shown on the left and for downflow on the right.

Once the flow reaches an approximately steady state, we can calculate well-defined average void fraction and liquid velocity profiles. In Fig. 4, we plot the average void fraction, computed by averaging over the y-direction and over several times after the flow reaches an approximately steady-state, as a function of x. Frame (a) corresponds to the upflow in the left frame of Fig. 2 and frame (b) to the downflow in the right hand side of Fig. 2. In addition to the profiles computed from the results of the simulations, we also plot two-fluid model predictions for the void fraction profile, obtained by solving Eqs. (1)–(3). Overall the agreement is reasonably good, particularly for the center of the channel. This is, however, not surprising since the average void fraction is the same in both cases. For the upflow, both the model and the simulation show a peak in the void fraction near the wall. The theoretical peak is, however sharper and closer to walls.

The average velocity profile, computed by averaging over the y-direction and over several times after the flow reaches an approximately steady state is plotted versus x in Fig. 5 for both cases, again with the theoretically predicted velocity profile superimposed. Since the bubbles "homogenize" the flow, resulting in steep gradients in the liquid velocity near the walls, the average flow rate is significantly lower than for the original laminar flow without bubbles. For the domain simulated here the profiles are relatively symmetric, but we note that preliminary simulations using a shorter channel (with the length equal to the width) frequently resulted in significant asymmetry in the velocity profile, that lasted for a long time. For the upflow, the model, using the original coefficients, overpredicts the velocity significantly but for the downflow the average values are closer.

The profiles predicted by the two-fluid model depend strongly on the various model parameters, such as the drag and the lift coefficient. In Figs. 4 and 5, we have used the values for the various coefficients in Eqs. (1)–(3) given by Azpitarte and Buscaglia (2003). These values are, however, derived for fully three-dimensional flows and there is no particular reason to expect the agreement with the present results to be very good. In the limit of zero Reynolds number, Eq. (4) is the drag for a solid sphere, not a bubble (since real bubbles are usually contaminated) and the drag of a two-dimensional cylinder is generally different than on a sphere with the same diameter. Furthermore, the drag in dense flows is generally higher than in dilute flows. To adjust the model

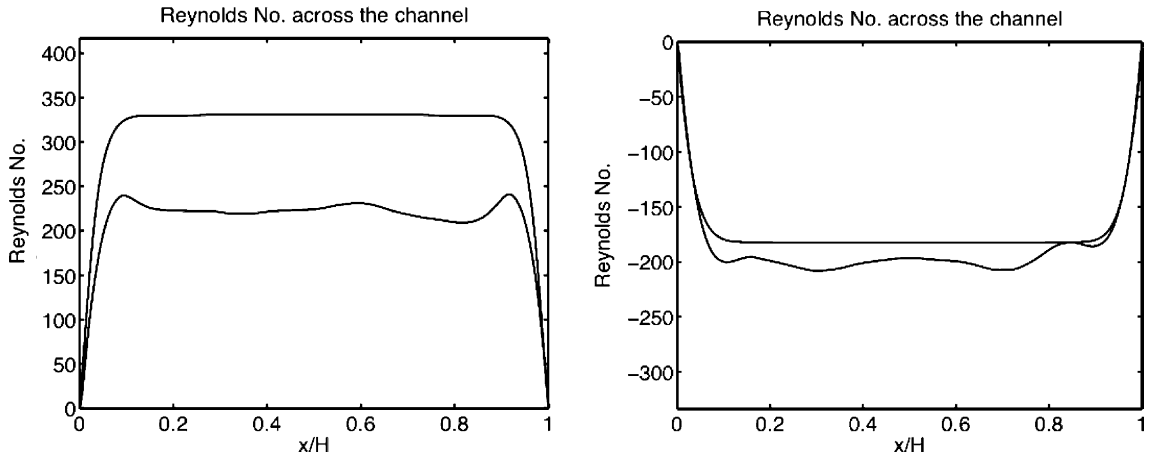

Fig. 5. The averaged velocity profile from the simulations and as predicted by the two-fluid model, using the original values for the model coefficients. Results for upflow are shown on the left and for downflow on the right.

coefficients it is natural to start by adjusting the drag coefficient. The average relative bubble Reynolds number (based on the channel width and the liquid properties) for the upflow case is $Re_r = 133.3$, which is very close to the relative bubbles Reynolds number found for bubbles rising in fully periodic domains with initially quiescent fluid ($Re_r = 124.9$). For the downflow we do, however, find a slightly lower value, $Re_r = 92.1$. The reason that the relative velocity is slightly lower for the downflow case is presumably that since the bubbles are pushed away from the walls, the effective void fraction in the center of the channel is slightly higher than that for the upflow and the periodic case (see Fig. 4). Using the relative velocity for the upflow case, and Eqs. (1), (4), and (5), we find that we can match the relative velocity by changing the coefficient in Eq. (4) from 24 to 18.3. This adjustment is well within the range of what we should expect. The original coefficient is for a solid sphere and for a bubble it should be replaced by 16, but the finite void fraction and the two-dimensionality result in a slightly higher drag than for an isolated, clean, spherical bubble. However, even if we match the relative velocity, we find that the liquid velocity profile is sensitively dependent on the lift coefficient (and the wall repulsion model) and it is difficult to adjust the model in such a way that the peaks in the void fraction distribution are at the correct location. The difficulty is that Eq. (2) for the velocity has no free parameters, so once the void fraction is determined the velocity is in effect also given. In Fig. 6 we plot the numerically obtained velocity and void fraction profiles for the upflow, along with several theoretical profiles obtained by adjusting the lift coefficient. For $C_L = 0.11$, we find that the average velocity matches the simulated results. The increase in the lift coefficient results, however, in wall peaks in the void fraction that are significantly closer to the wall than found in the simulations. The location of the wall peak is likely to be determined by the size of the bubbles, and we note that the wall peak predicted by Antal et al. was also closer to the wall than the wall peak in the experimental data that they compared their predictions with. The difficulties in adjusting the model to exactly match the void fraction peak for upflow, raise interesting questions about whether there are aspects of dense flows that cannot be captured by the present model. A more sophisticated wall-repulsion model has recently been introduced by Moraga et al. (2004), but we have elected

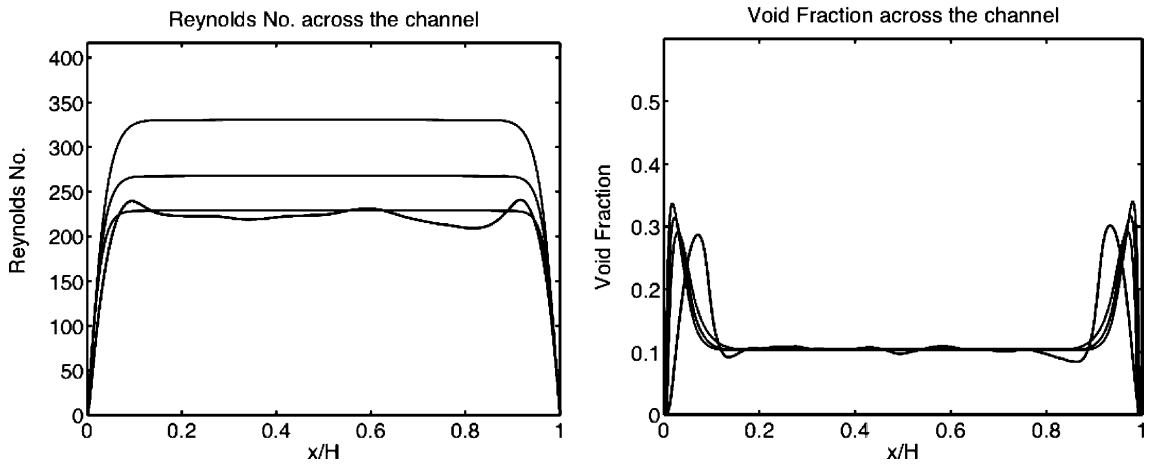

Fig. 6. The effect of adjusting the model coefficients for the upflow case. The result from the full simulations, along with three profiles obtained by the two-fluid model are shown. The averaged fluid Reynolds number is on the left and the void fraction is on the right. The values of the leading numerical coefficient in Eq. (5) are 24, 18.3, 18.3 and the lift coefficient is 0.05, 0.10, 0.14, for the three different model profile shown.

to postpone an investigation of how it improves the results until we examine a fully three-dimensional system.

Although we have not been able to match both the void fraction and the velocity profiles from the simulation and the two-fluid model results perfectly, we have examined how the model, both with the original and the ''best'' values from Fig. 6, does for a number of other cases. In Fig. 7 we show the effect of reducing the gravity by a factor of two, for both the upflow and the downflow,

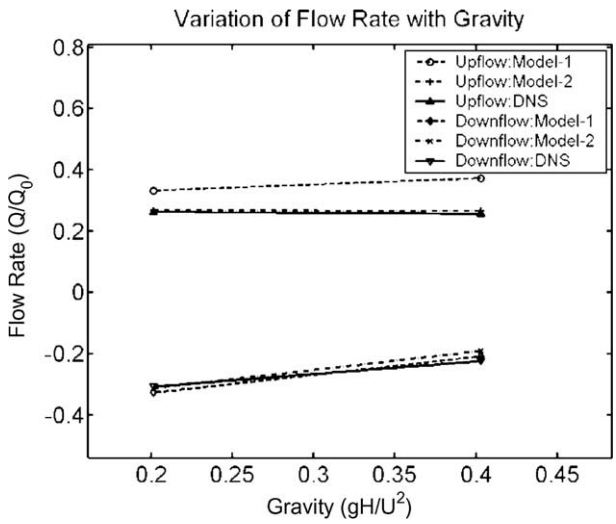

Fig. 7. Total flow rate for different values of gravity as predicted by the full simulations and a two-fluid model with two sets of model parameters.

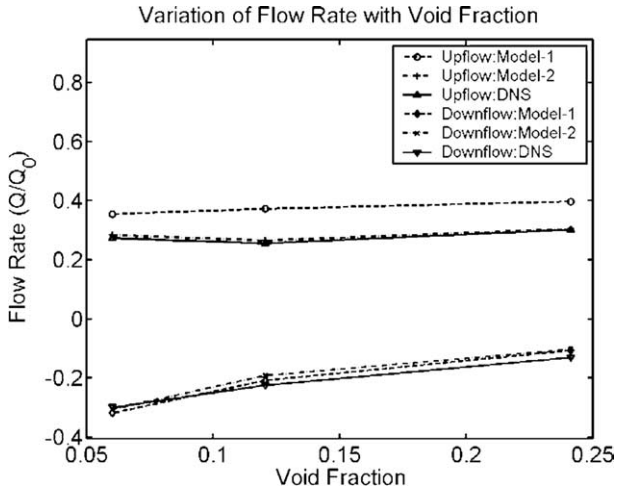

Fig. 8. Total flow rate for different values of the void fraction, changed by changing the number of bubbles, as predicted by the full simulations and a two-fluid model with two sets of model parameters.

by plotting the total through flow versus gravity. In addition to the results from the DNS (solid line), we show model predictions for the original parameters used in Figs. 3 and 4 (“model 1”) as well as for the “best” set from Fig. 6 (“model 2”). For the downflow the effect of varying the parameters is very small, but for the upflow the model predictions is significantly improved by using the new values.

A similar test for the effect of the void fraction, changed by changing the number of bubbles in the channel is shown in Fig. 8. Here again the downflow shows good agreement between the DNS

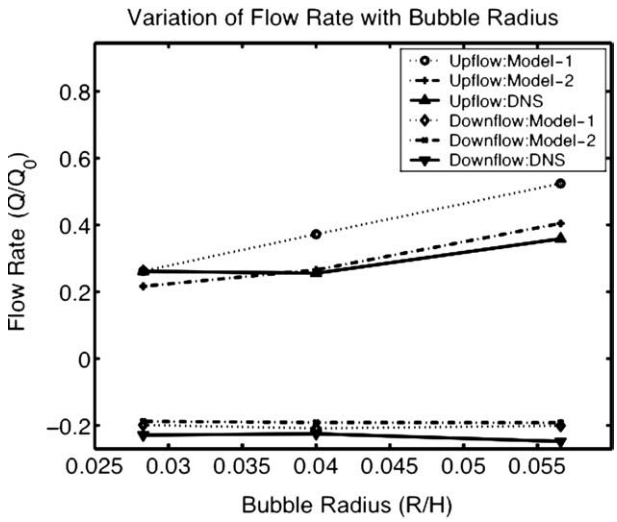

Fig. 9. Total flow rate for different bubbles sizes, but the same void fraction as predicted by the full simulations and a two-fluid model with two sets of model parameters.

results and the predictions of the two-fluid model, for both sets of modeling parameters. For the upflow case the model with the adjusted parameters captures the DNS results nearly perfectly.

Finally, we have used bubbles of different sizes, keeping the void fraction the same by changing the number of bubbles. The results are plotted in Fig. 9. Here again the downflow results are all relatively close, and the adjusted model parameters bring the two-fluid predictions in closer agreement with the DNS results. The agreement is, however, not quite as good as in Figs. 7 and 8, suggesting that either the simple adjustment that we made in the drag law, Eq. (4), may not capture the size effect well, or that the lift coefficient may need to be readjusted again.

5. Conclusions

The study reported here is obviously only a modest first step in bridging the gap between direct numerical simulations of multiphase flows and two-fluid models. We have chosen to look at bubbly flows in a very simple geometry since this flow has been studied extensively experimentally and two-fluid modeling of this setup has been very successful. While we have only looked at two-dimensional flows here, the reasonably good agreement obtained (with relatively minor adjustment of the model to account for the two-dimensionality) confirms that it is possible to simulate multibubble systems that are sufficiently large so they are well described by two-fluid models. While this is perhaps not too surprising, it is nevertheless not a completely trivial issue either. We would normally not expect a system of two or three bubbles, for example, to be accurately modeled by averaged models. And, indeed, we found that simulations using shorter channels (with the length equal to the width) resulted in large asymmetries. Two-fluid models are usually derived under the assumption that the system under consideration is either ''infinitely large'' or, more properly, that the model describes the behavior of an ensemble of infinitely many realizations. Thus, the question is, how large of a system is large enough? As direct numerical simulations are generally limited to relatively small systems, finding that the domain of validity extends to those systems that can be computed easily, allows us to use the simulations results for calibration of the models. And as our results showed, adjusting the model parameters for one case, leads to a relatively good predictions when we change the governing parameters—at least within the range of parameters examined here.

Acknowledgment

This study was funded by the Department of Energy, Grant DE-FG02-03ER46083.

References

Antal, S.P., Lahey, R.T., Flaherty, J.E., 1991. Analysis of phase distribution in fully developed laminar bubbly two-phase flow. Int. J. Multiphase Flow 17, 635–652.

Azpitarte, O.E., Buscaglia, G.C., 2003. Analytical and numerical evaluation of two-fluid model solutions for laminar fully developed bubbly two-phase flows. Chem. Eng. Sci. 58, 3765–3776.

Crowe, C., Sommerfeld, M., Tsuji, Y., 1998. Multiphase Flows with Droplets and Particles. CRC Press.

Drew, D.A., Passman, S.L., 1999. Theory of Multicomponent Fluids. Springer.

Esmaeeli, A., Tryggvason, G., 1999. Direct numerical simulations of bubbly flows. Part II—Moderate Reynolds number arrays. J. Fluid Mech. 385, 325–358.

Kaneda, Y., Ishihara, T., Yokokawa, M., Itakura, K., Uno, A., 2003. Energy dissipation rate and energy spectrum in high resolution direct numerical simulations of turbulence in a periodic box. Phys. Fluids 15.

Moraga, F.J., Drew, D.A., Lahey Jr., R.T., 2004. The modeling of wall-induced forces in two-fluid model simulations of a bubbly flow. In: 5th International Conference on Multiphase Flow, ICMF'04 Yokohama, Japan, May 30–June 4, Paper No. 186.

Tryggvason, G., Bunner, B., Esmaeeli, A., Juric, D., Al-Rawahi, N., Tauber, W., Han, J., Nas, S., Jan, Y.-J., 2001. A Front Tracking Method for the Computations of Multiphase Flow. J. Comput. Phys. 169, 708–759.